We are IntechOpen, the world's leading publisher of Open Access books Built by scientists, for scientists

5,300
Open access books available

130,000
International authors and editors

155M
Downloads

Our authors are among the

154
Countries delivered to

TOP 1%
most cited scientists

12.2%
Contributors from top 500 universities

CLARIVATE ANALYTICS BOOK CITATION INDEX INDEXED

WEB OF SCIENCE™

Selection of our books indexed in the Book Citation Index in Web of Science™ Core Collection (BKCI)

Interested in publishing with us?
Contact book.department@intechopen.com

Numbers displayed above are based on latest data collected.
For more information visit www.intechopen.com

9

SLOT OPTICAL WAVEGUIDES SIMULATIONS & MODELING

Muddassir Iqbal[1], Z. Zheng[2] and J.S. Liu[2]
1. National University of Science & Technology, H-12, Islamabad, Pakistan
2. Beihang University Beijing China.

1. Introduction

In this chapter we will discuss about slot optical waveguides analysis using finite difference time domain (FDTD) algorithm. SOI slot optical waveguides invented in 2004, by Lipson at Cornell nanophotonics center [1], and experimentally demonstrated by them in forming complex nano-structures [2]. Nanophotonics group at Cornell surprised photonics researchers by discovering structure geometry; where light can be confined inside low index slot region due to electric field discontinuity.

The name slot waveguide comes from its physical shape i.e. a low index slot surrounded by two high index slabs. Slot waveguide structure has gained significant interests and importance due to its potential applications in nanophotonics especially light on chip circuits. In most basic single slot waveguide structure a high-refractive-index material is used to guide light through a low-refractive-index material. The waveguide structures are capable of guiding and confining light in such a way that very high optical intensity is obtained in a small cross-sectional area or gap filled with any material of sufficiently low refractive index, relative to the remainder of the structure. (Figure 1 is a top view of a slot waveguide structure)

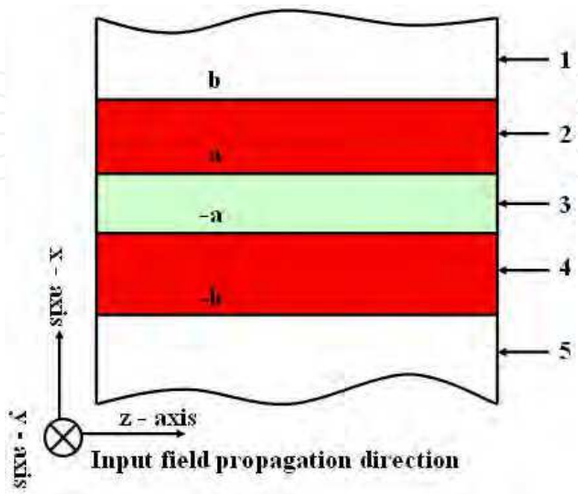

Fig. 1. Basic single slot waveguide structure.

Referring figure 1, the slot waveguide structure comprises of slabs (No.2 & 4) having high index of refraction and a slot (No.3) formed in between, which have a relatively low index of refraction. The cladding region (No.1 &5) comprises of low refractive index material or same material as used for the slot region. The analytical solution for the transverse E-field profile E_x of the fundamental TM Eigen mode of the slab-based slot waveguide is [1]:

$$E_x(x) = A\begin{cases} \frac{1}{n_s^2}\cosh(\gamma_s x); |x| < a \\ \frac{1}{n_H^2}\cosh(\gamma_s a)\cos\left[\kappa_H\left(|x|-a\right)\right] + \frac{\gamma_s}{n_s^2\kappa_H}\sinh\left[\kappa\left(|x|-a\right)\right]; a < |x| < b \\ \frac{1}{n_c^2}\left\{\cosh(\gamma_s a)\cos\left[\kappa_H(b-a)\right] + \frac{n_H^2\gamma_s}{n_s^2\kappa_H}\sinh(\gamma_s a)\sin\left[\kappa_H(b-a)\right]\right\}\exp\left[-\gamma_c\left(|x|-b\right)\right]; |x| > b \end{cases} \quad (1)$$

κ_H is the transverse wave number in high refractive index slabs. γ_χ is the field decay coefficient in the cladding. γ_σ is the field decay coefficient in the low refractive index slot waveguide. The constant A can be narrated mathematically as follows [1, 2]:

$$A = A_0\frac{\sqrt{k_0^2 n_H^2 - k_H^2}}{k_0} \quad (2)$$

A_0 is an arbitrary constant. $\kappa_0 = 2\pi/\lambda_0$ is the vacuum wave number. Figure 2 below displays e-field distribution in a basic single slot structure.

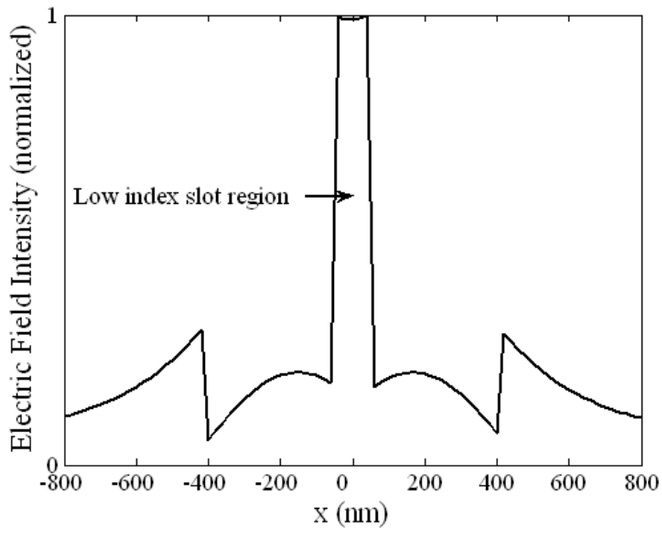

Fig. 2. High confinement of light in low index slot region.

The structure provides strong confinement in low refractive index materials, which rely on the discontinuity of the electric field perpendicular to the interface between materials with low and high refractive index. In such a case, the strongest electric field amplitude lies in the material with low refractive index. Due to the large index contrast at interfaces, the normal electric field undergoes a large discontinuity, which results in a field enhancement in the

low-index region. If refractive index of slot is denoted by n_l sandwiched between two slabs (refractive index denoted by n_H), e-field enhancement in low-index region is of the order of n_H^2 / n_l^2 . In order to measure the optical field confinement, the optical confinement factor can be defined as the fraction of power confined and guided in the interested regions [3]:

$$\Gamma = \frac{\int_{\text{Regions}} \text{Re}\left(E \times H^*\right).\hat{z}dxdy}{\int_{total} \text{Re}\left(E \times H^*\right).\hat{z}dxdy} \tag{3}$$

Where *E* and *H* are the electric and magnetic field vectors. The integrals are calculated inside the interested regions and the entire cross section regions. Optical field confinement in this chapter has been calculated based on the theory [1, 3]. Simulation of slot waveguide geometry leads to high confinement of light in low index slot region (figure 2 shows high confinement of light in low index slot).

Experimental demonstration of guiding and confining light in low index waveguides by Lipson [2], led other researchers to demonstrate slot waveguide based complex structures [4, 5]. High power confinement can also be achieved in asymmetric slot waveguides [6]. Power confined inside slot structure can be optimized by adjusting the geometry of slot and slabs [7, 8]. N. N. Feng demonstrated slot waveguide coupling capability with conventional waveguides [9]. Barrios, and Passaro proposed slot waveguides for sensing [10, 11]. Beyond single slot structure people are interested in multiple slot structure confining optical field in nanometer-thin low-index media with very high optical confinement factor [3]. Slot waveguides capable of confining high intensity electric field hence became an interesting topic of researchers to simulate and demonstrate nonlinear slot structures [12, 13]. Other than dielectrics, slot waveguides had been demonstrated by Lipson and Atwater in metals as well [14, 15]. While exploring characteristics of single and multiple slot structures, comparable light confinement in low refractive index contrast slot structures have been demonstrated [16]; a novel photonics displacement sensor based upon multiple slot waveguide structure has been proposed [17].

2. Slot Structure Analysis

As mentioned earlier, in a slot structure electric field discontinuity at the boundary between the high and low index regions results in high E-field confinement inside low index slot. Slot waveguide structure had been simulated using OptiFDTD simulation software from Optiwave Company. Finite difference time domain method (FDTD) uses a brute force discretization of Maxwell's equations. The structure is discretized using a uniform grid and the derivatives in Maxwell's equations are replaced by finite differences. The grid size used is very important, a small grid size is required to get accurate results. However using more grid points results in longer calculation times. The grid size also imposes an upper limit on the time step that can be used, because of stability requirements. FDTD can handle almost any 2-D or 3-D structure (in theory), but computation time and memory requirements limit the size of the problem that can be handled. It has been explored by us that 3dB waist of input plane and mesh size has a profound effect on the output. Hence it was decided that for the nanosize slot optical waveguide analysis using OptiFDTD, a grid size of 10 nm is to

be used along x- and y-axis. However grid size in z-direction can be changed to get quicker results, it does not have profound impact on results. Sources are placed inside the waveguide to excite the waveguide mode and detectors are placed above to detect the output signal and power. Appropriate boundary conditions (e.g. PML) are used to avoid reflections at the boundaries of the computational domain and model open structures.

In a basic slot waveguide structure cladding, substrate and slot are of fused silica, whereas slabs comprising of silicon. Slot structures are ignited by placing a continuous wave (C.W.) input plane of 1.5 μm wavelength, direction of flow is in z-axis. Three observation planes had been placed at a distance of 0.5 μm, 1 μm and 1.5 μm. The observation planes were centered with the slot structure center in x-axis and y-axis. E-field distributions in spatial domain are shown in figure 3.

E-field distribution at respective propagation distances had also been checked, a combined plot at different propagation lengths is shown in figure 4 below. It was found that E-field in slabs and cladding for a propagation distance of 1 μm and 1.5 μm is at a monotonous decrease then at 0.5 μm distance and seems more stable. Hence in order to get stable results, it was decided to propagate signal for longer distance.

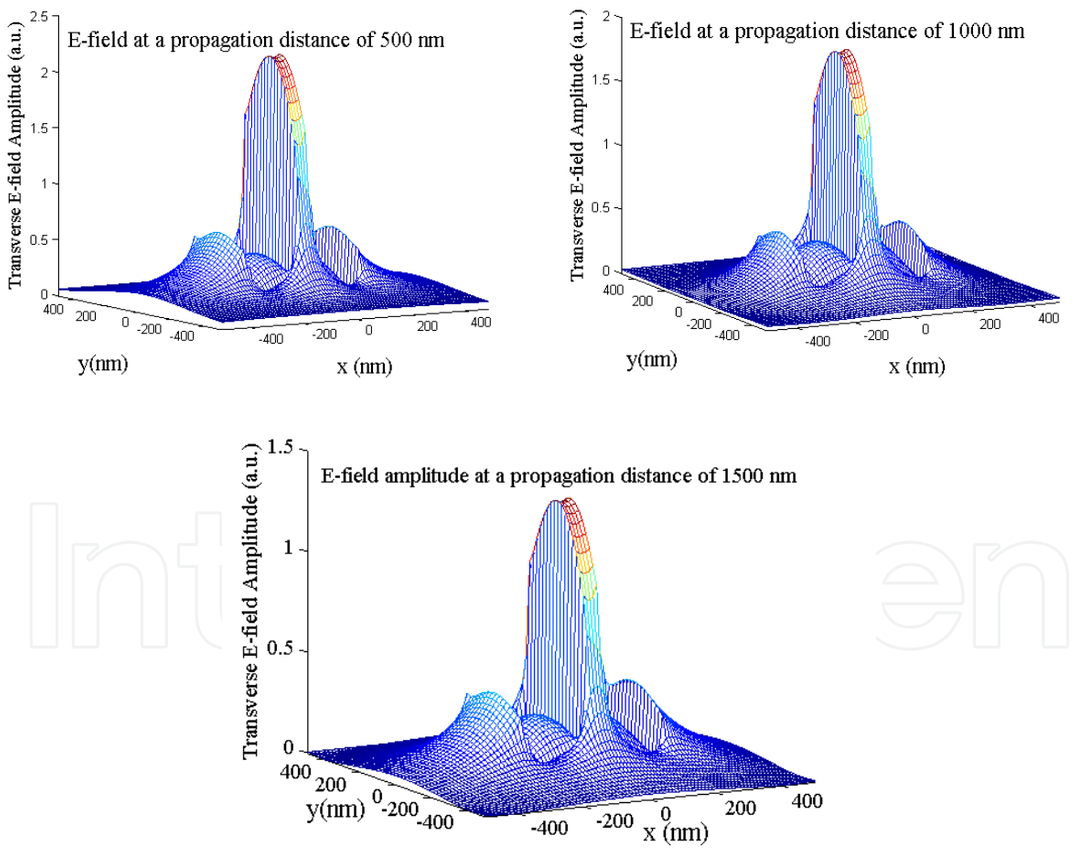

Fig. 3. E-field distribution in slot structure at different propagation distances.

However OptiFDTD ver. – 5.0 has less memory and longer simulations made the memory buffers overflow, hence most of those simulations crashed unanimously.

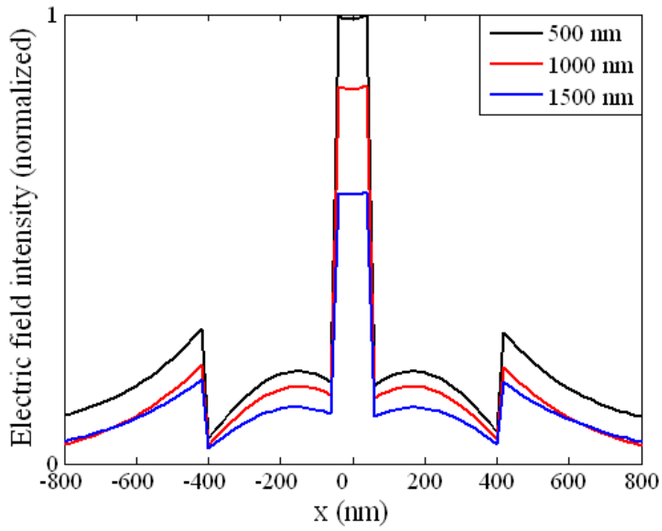

Fig. 4. Modes for single slot structure at various propagation distances.

Power confinement factor in the slot structure has been checked and found in accordance with the previous work [1].
In an extended check of power confinement factor in slot waveguide structure, the refractive index in slot region varied from 1.44 till 1.50 with a step size of 0.005. High index slabs refractive index was kept constant at 3.48, cladding and substrate refractive index kept constant at 1.44. It was found that power confinement factor varied (increased / decreased) as per the ratio, n_H^2 / n_l^2 .

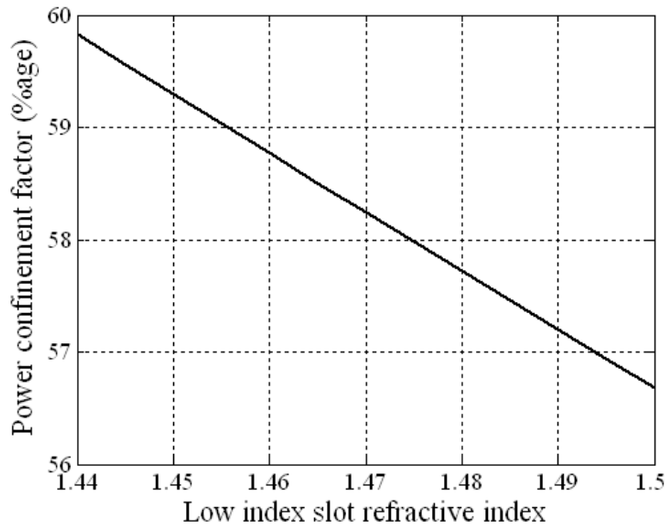

Fig. 5. Slot region power confinement dependence on refractive index.

In order to simulate complex structures, double slot structure was simulated, which was a step towards complex structures designing and simulation. A double slot structure has been simulated, where both slots of 50 nm width each are separated by a central high index slab of 100 nm width and surrounded by two 180 nm wide high index slabs. Initially it was thought that double slot structure designing is not a big issue, as it is just adding one more slot of suitable width in the waveguide structure (see figure 6). However, later it was learnt through various simulations that adding another slot of any width could not solve the problem. It requires proper width and placement of slot, as center slab width is dependent upon the placement of extra slot. Center slab width determines the amount of coupling occurring in between both the slots. The coupling effect between both slots does have an effect on power confinement factor in the low index slot region. This coupling effect determines the amount of power confined inside low index slot regions; moreover it has also been found that the center slab width can be related with the power confinement factor inside low index slot regions.

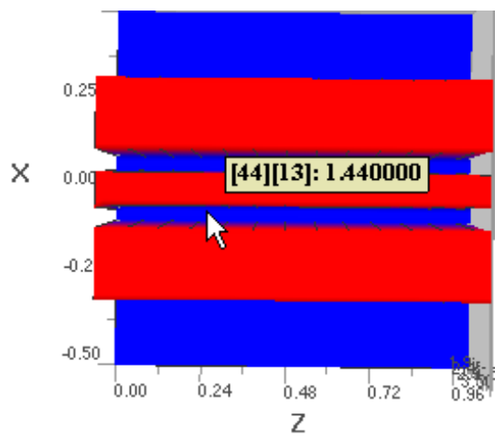

Fig. 6. Double slot structure (refractive index based view).

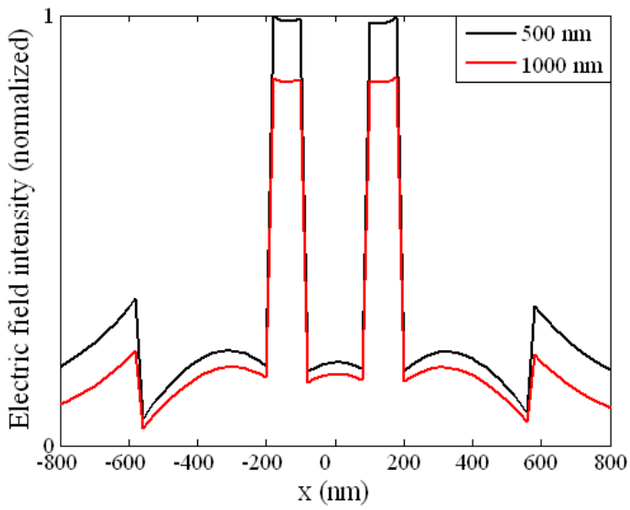

Fig. 7. E-field distribution for double slot structure at 0.5 μm & 1 μm propagation distance (low index slots R.I. = 1.44, high index slabs R.I. = 3.48, cladding & substrate R.I. = 1.44).

Further exploration of double slot structure had been done by using different refractive index materials in both low index slots. The results proved that power confinement and E-field confinement is dependent upon the contrast ratio. The more the contrast ratio between low index slot and high index slabs; the more the power confined inside low index slot region. In the current work, refractive index for left slot was 1.5, right slot was 1.44; high index slabs refractive index is 3.48. E-field distribution at a propagation distance of 0.5 μm, 0.75 μm, 1 μm, and 1.5 μm are displayed in figure 8. Referring figure 5, for a single slot structure power confined inside low index slot region follows the refractive index contrast ratio between high index slabs and low index slots. It has been found that in case of double slot structure, power confined inside low index slot regions is affected by the coupling effect as well. Coupling between low index slot regions is mainly dependent upon central high index slab width. This effect has been studied in detail, and is of use in attaining fruitful results.

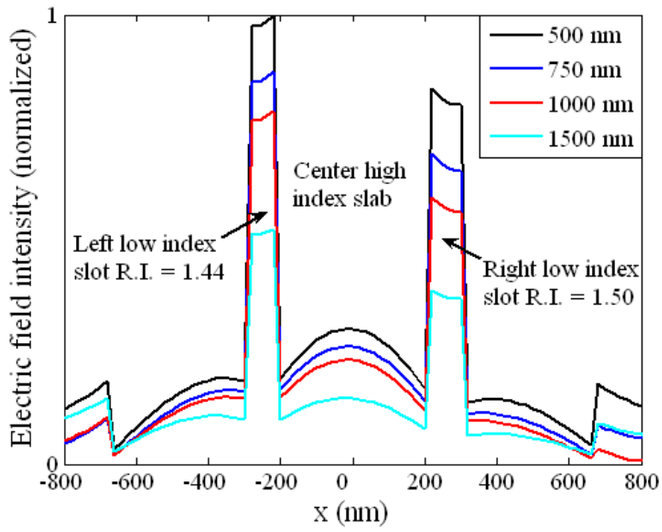

Fig. 8. E-field distribution for double slot structure with different R.I. at 500 nm, 750 nm, 1000 nm & 1500 nm propagation distance (high index slab R.I. = 3.48, cladding & substrate R.I. = 1.44).

E-field inside both slots for both distances had been analyzed for phase shift. Phase shifts had been calculated at various parametric values, minute difference in phase shift indicates its non-existence.

In another example, the double slot structure (ref. figure 6 & related details) has been repeated with cladding comprising of air. Power confined inside low index slot regions increased with a subsequent decrease of power confinement in external slabs. E-field distribution at 500 nm and 1000 nm propagation distances are shown in figure 9 below.

It was found that E-field confinement in the slot with comparatively high index of refraction is less than the other slot. This behavior of light confinement inside low index slot region is directly related to the slot and slab refractive index contrast ratio; and has already been discussed.

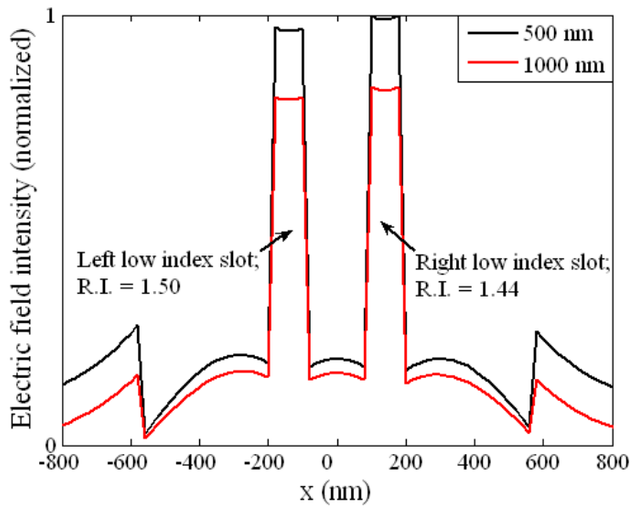

Fig. 9. Modes for double slot structure with different R.I. (cladding is air).

3. SOI Multiple Slot Structures Explored for Sensor Applications

In case of double slot structure, power confined inside low index slot regions (combined and individually) is dependent upon the center slab width. Several values have been taken at slot width 50 nm each; external slabs width 180 nm each slots and slabs height 300 nm each. Power confinement factor inside low index slot regions was found dependent upon center slab width.

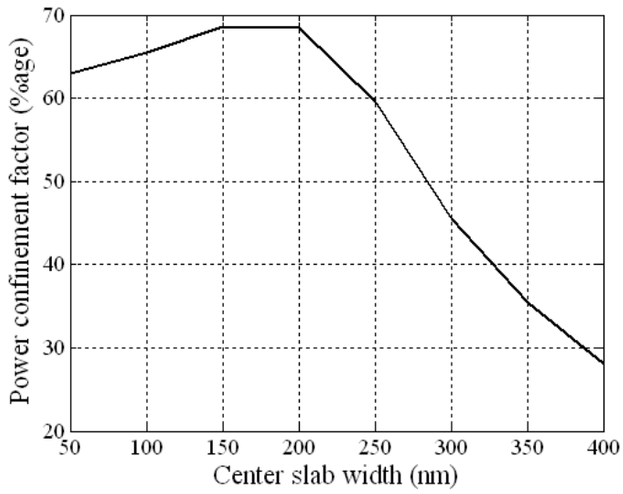

Fig. 10. Dependence of power confinement factor in double slot structure upon center slab width.

In an extended check it was found that power confined inside low index slot regions of width 50 nm each is maximum for a center slab width ranging from 150-200 nm. Center slab has a profound impact in a double slot structure on power confinement factor in low index

slot region. E-field amplitude also varies for slots with different refractive index. Power confinement factor ratio between slots, normalized values of power confined in center slab and E-field amplitude ratio in slots is shown in figure 11 [17]. In order to check the variation in power confinement factor due to shift in refractive index of slots; power confinement ratio in slots is plotted for a shift in refractive index values by 0.005. Refractive index value in left slot was changed from 1.44 till 1.5 with a step of 0.005, whereas refractive index value in right slot kept constant at 1.44. Ratio in power confinement factor between both slots was calculated and it was found that the peak is shifting gradually with shift in refractive index. The results have proven the effect of shift in refractive index on power confined in low index slot regions. Numerically calculated power confinement factor ratio for shift in refractive index shows a promising behavior for probable usage in sensor systems. However the use of single slot structure in sensor systems does require a mechanism to sense the shift in modal effective index, which had been studied by others. Double slot structure showed a way to use the slot structure in sensing mechanisms; most probably by calculating and observing the shift in power confinement factor / power confinement factor ratio. The shift in power confinement factor of low index slot regions under the action of cantilever [10] type movement by central high index slab has been exploited by us in proposing double slot structures usage in forming sensor systems. This effect is discussed in detail in further half of this chapter.

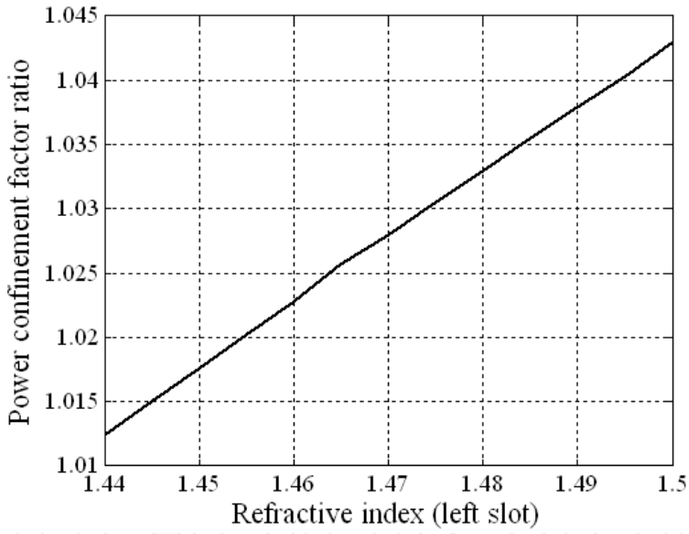

Fig. 11. Power confinement ratio in diff. refractive index slots dependence upon shift in refractive index of one slot.

Variation of refractive index only in left low index slot region only showed a profound impact upon power confinement factor ratio between both low index slot regions. Extensive research work done in this direction, so as to utilize the shift in refractive index of low index slot region (one or all in a multiple slot structure); a center slab width of 165 nm was chosen for extended extensive analysis. The reason of choosing 165 nm center slab width was that; at this center slab width coupling between low index slot regions was comparatively less. The results could help us in ascertaining the postulate that shift in refractive index of any of the low index slot region do have a profound impact on the power confinement inside low

index slot regions. Refractive index in left low index slot region shifted from 1.5 till 1.48 with a step size (Δn) of 0.005. Minute shift in refractive index; which is possible due to temperature, pressure, chemical, and mechanical, or may be due to several other reasons not mentioned here; had a profound impact on power confinement factor and its ratio between both low index slot regions. Prominent shift in low index slot regions power confinement factor formed a basis of thinking to propose double slot optical waveguide structure for use in sensor applications. Power confinement ratio between both low index slots as a function of center slab width and refractive index is plotted in figure 12:

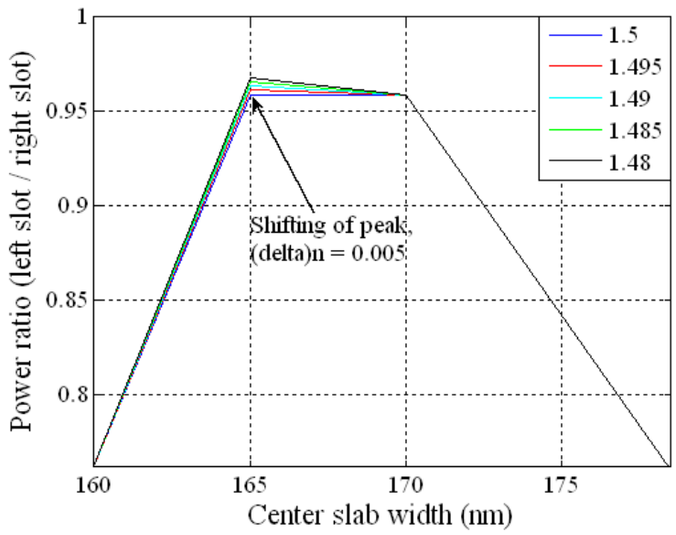

Fig. 12. Shift in power confinement ratio in low index regions due to change in refractive index.

In one of the research work related to proposing double slot structure in sensor mechanisms, numerical calculations were performed for a center slab width varying from 10 nm till 400 nm. Followed by power confinement factor ratio dependence upon shift in refractive index of low index slot region. Refractive index of right slot is kept constant at 1.44, whereas refractive index of left slot was varied from 1.44 till 1.5 with a step size of 0.005. Power confinement factor ratio was calculated by dividing the power confined in right slot with power confined in left slot for a propagation length of 1 μm. Power confinement ratio between both low index slot regions is maximum at a center slab width of 20 nm. Hence the point with center slab of 20nm width was chosen for power ratio check. For a 20 nm width of center slab, coupling between both low index slot regions is better than at center slab width of 165nm. This time power confinement factor ratio at a center slab width of 20 nm was checked, where power confinement factor inside low index slot regions is more due to increased coupling. Shift in refractive index of either of the low index slot region showed a profound impact on power confinement factor ratio. The prominent change in power confinement factor (can also be termed as confinement loss) is a contributing factor leads to proposing double slot structure for use in sensing mechanisms. Change in power confinement factor ratio indicates that a slight shift in either of the low index slot regions refractive index shows a promising change in power confinement factor ratio.

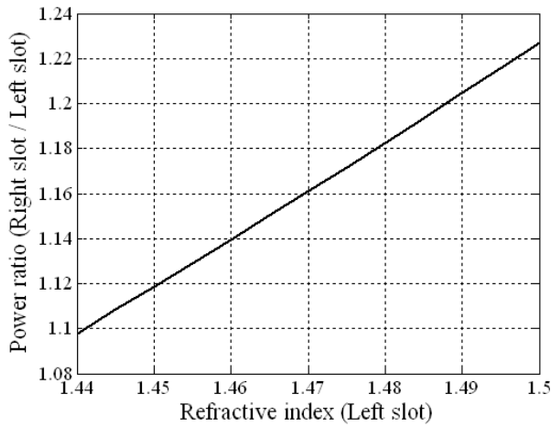

Fig. 13. Shift in power confinement ratio dependence on left low index slot R.I. (center slab width 20 nm).

Before considering power confinement / loss mechanism in double slot structure for use in sensor mechanisms, it was necessary to investigate if change in power confinement factor is dependent upon some other parametric values. Several checks have been done, in one case where refractive index in both slot regions is 1.44, detailed analysis of boundary conditions effect upon power confinement factor ratio has been done for a center slab width of 162 nm. Perfectly matched boundary conditions are used with number of layers ten and twenty. Power confinement factor ratio (right slot/left slot) at various propagation distances are plotted in figure 14 below.

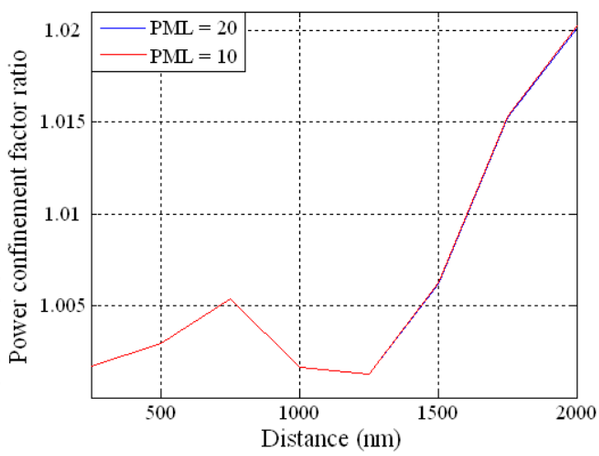

Fig. 14. Power confinement factor ratio between slots dependence on Perfectly Matched Layers boundary condition.

Later part of this subsection indicates that number of PML layers does not have profound impact on power confinement factor, hence we have kept the number of PML layers in all of our simulations to be 10. It is apparent from both the results that power confinement factor ratios are around the value of one. As the propagation conditions (boundary conditions &

input conditions) in both slot regions is same, hence ideally the ratio should be one or in close proximity of one.
Comparison between the results of both conditions, like PML=10 and PML=20 had been carried out. Power confinement factor error ratio has been plotted in figure 15. The error ratio has been taken for difference in power confinement ratio at PML-10 and PML-20 divided by actual ratio at PML-10. The error ratio is at monotonous increase hence it seems following the general conditions of error analysis.

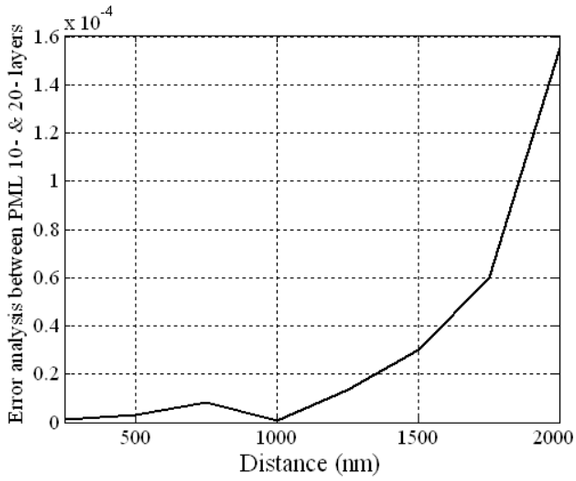

Fig. 15. Power Confinement factor ratio comparison (PML = 10 & PML = 20).

Hence it was found that power confinement factor is mainly dependent upon shift in refractive index, and shift in center slab width (double slot structure).

4. Low contrast Double Slot Structure based Optomechanical Sensor [18]

The structure is based on basic double slot structure. A head start introduction of proposed optomechanical sensor is that two low index slots of hard material dipped in a cladding of high index compressible material (suitable to term as fluid), where slots have fins on top and can move inside high index cladding under the action of an external force. Three slabs comprising of high refractive index fluid, two slots (50nm wide) of low refractive index solid material, in present work it is SiO_2 (R.I.=1.44). The cladding and substrate also comprised of SiO_2. Slabs comprising of commercially available high refractive index fluid; Gallium Halide (R.I. = 2.31) [19]. Melting point of fused silica (to be used in forming low index slots) is ~1371^{o}C. Trihalides where Gallium is in the +3 oxidation state are Gallium Fluoride (GaF_3), Gallium Chloride ($GaCl_3$), Gallium Bromide ($GaBr_3$), and Gallium Iodide (GaI_3). Other than GaF_3 having melting point above 1000^{o}C, all other three halides ($GaCl_3$, $GaBr_3$, and GaI_3) melting point is 78^{o}C, 122^{o}C, and 212^{o}C respectively. Hence it seems technically reasonable to use fused silica based slots inside a Halide based slab.
Block diagram of proposed optomechanical sensor is shown in figure 16.
Essential assumptions in double slot structure are:

(a) Slabs comprising of high refractive index fluid.
(b) Slots body is dipped inside the slabs, there are fins on top of slots body; which are visible out of the slabs and are exposed to atmospheric conditions.

(c) Cladding is of air.

(d) Slots width remains same, the distance in between slots is varied subject to change in atmospheric conditions like temperature and pressure on the fins. As the slabs comprise of fluid, hence slots can move easily inside the slabs. Increase or decrease in central slab width (in between slots) is added into outer slabs equally

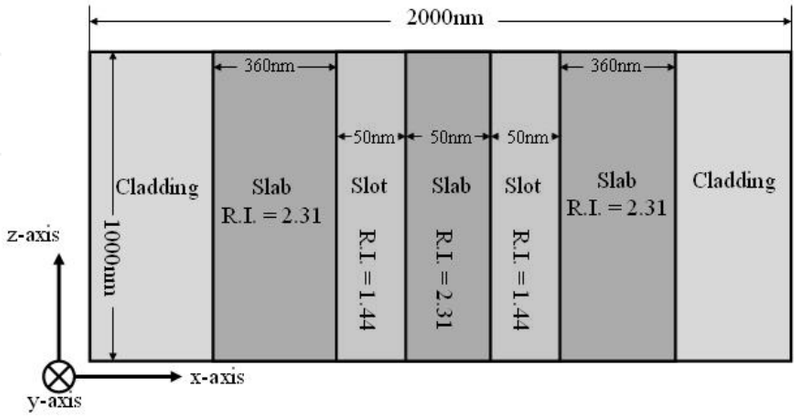

Fig. 16. Top view (z-cut) of compressible material based slot structure.

Power confinement factor in basic single slot structure (where slab refractive index is 2.31 and slot refractive index is 1.44) is investigated at various structure heights ranging from 300 nm till 500 nm with a step size of 10 nm. It has been found that for a propagation distance of 1000 nm, power confinement factor in slot waveguide shows a monotonous increase till structure height of 380nm, later on it shows a monotonous decrease till 500nm. Further analysis proved that a structure height of 410 nm is an optimized height. Hence for the current work in this section, structure height was kept at 410 nm.

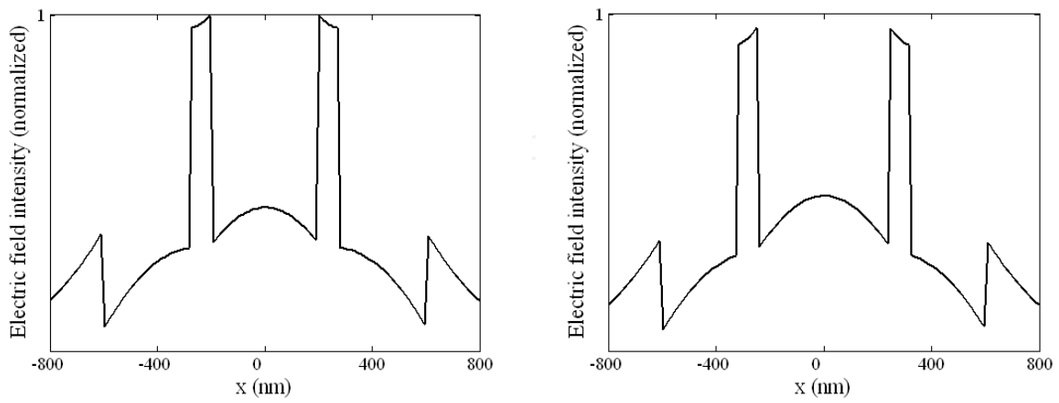

Fig.17. E-field intensity dependence upon central slab width; (a) 250 nm; (b) 300 nm.

As an example we can see that; for a case where central slab width between both slots is 300 nm and 250 nm. E-field intensity (see figure 17), E-field lines (see figure 18) and power confinement factor in low index slot region changes considerably.
The contrast ratio in present structure is considerably low, however we can see acceptable power confinement factor inside low index slot regions. E-field lines in both the cases (central slab width of 250 nm, and 300 nm) were checked. It was found that power confinement inside low index slot regions occurred due to electric lines discontinuity, plotted in figure below:

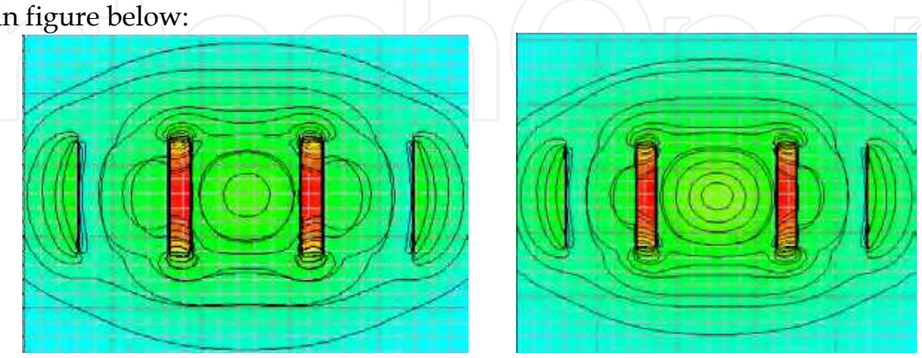

(a) (b)

Fig. 18. E-field lines at a central slab width of; (a) 250 nm; (b) 300 nm.

Power confinement factor in a low index slot has been calculated and plotted in figure 19 below. A monotonously decreasing curve was found for various widths of central slab (comprising of high index compressible material) between the slots (comprising of low index hard material). In this case power confinement factor is depending upon center slab width.

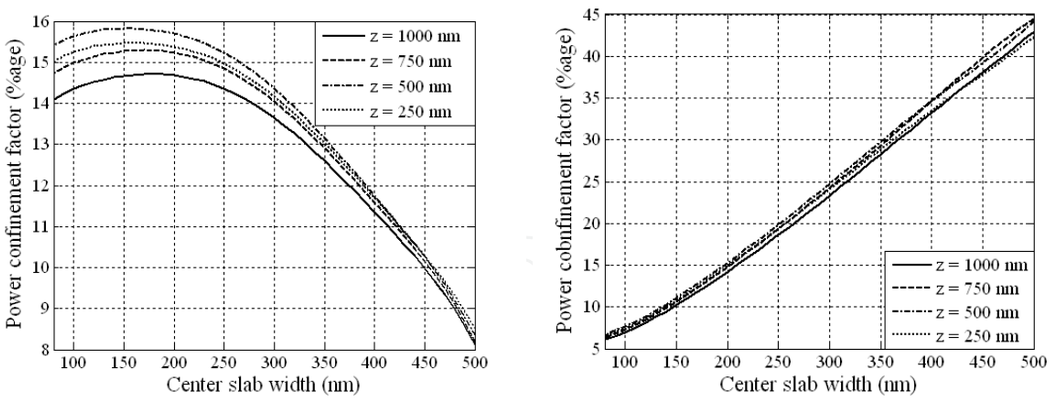

(a) (b)

Fig. 19. Power confinement factor dependence upon central slab width; (a) low index slot; (b) central high index slab.

In a careful review of the power confinement characteristics of the fluid based photonics waveguide sensor reveals that; power confinement in low index slot regions is at a monotonous decrease for a central slab width ranging from 300nm till 650nm and is as follows:

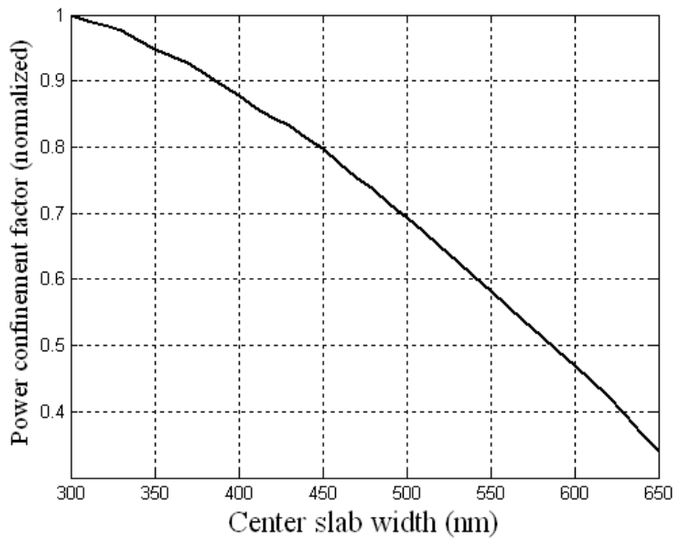

Fig.20. Normalized power confined in low index slot region.

The sensitivity of the sensor can be calculated by finding the slope of un-normalized deflection curve $((y_2-y_1)/(x_2-x_1))$, however the material sensitivity towards deflection is also required. The material sensitivity depends upon the nature of sensor requirement and its constituents. Shift in power confinement factor in this embodiment came out to be 0.435/nm.

5. Glass based Multiple Slot Structure Sensor Systems

Further to our work in last section, it was thought of that a simple and easy to realize double slot structure should be explored for sensing applications. Inspired from the work by Barrios [10], glass based double slot structure has been realized. The structure composition is that glass slabs are placed on glass substrate. Both low index slot regions and cladding is of air, for simplicity and to be practical we may say that low index slot regions and cladding is of compressible low index material. Before starting work on the proposed structure of glass and air based double slot structure, power confinement factor in glass and air based single slot structure has been investigated. Deviating from the contrast ratio of SOI slot optical waveguide, where contrast ratio is 2.42, we were thinking of realizing a structure with contrast ratio of 1.65. In a basic structure, 500 nm high, 50 nm wide single slot comprising of air, surrounded by glass slabs (R.I. = 1.65). The structure is resting on glass substrate, cladding is of air. E-field in y-cut and E-field distribution shown in figure 21 are in agreement with the basic slot structure theory [1]. High E-field confinement was found in the low index slot region.

Power confinement factor percentage inside low index slot region found out to be 9.1%. In order to enhance the power glass based double slot structure was realized. Two 500 nm high, 50 nm wide air based slots separated using a 50 nm wide glass slab, surrounded by 360 nm glass slabs. Whole structure resting on glass substrate, cladding comprising of air.

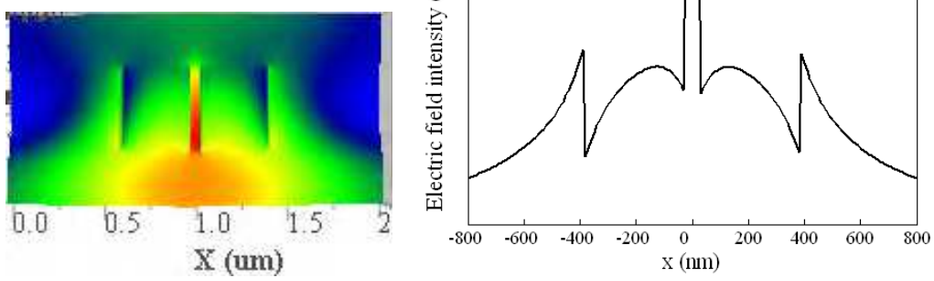

(a) (b)

Fig. 21. (a) E-field distribution; (b) E-field intensity; glass based single slot structure.

E-field distribution in y-cut and E-field intensity is shown in figure 22 (a) and (b) respectively. E-field distribution and power confinement for glass based structure had also been checked for the case where slabs comprising of glass (R.I. = 1.65); cladding, substrate & slot comprising of air. In other words for a single slot structure there are two glass slabs inserted inside an air based wafer at the requisite

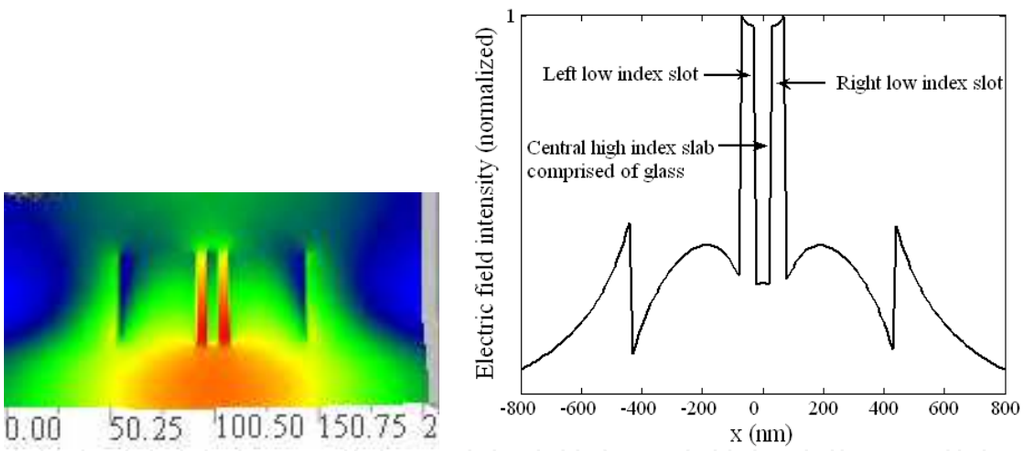

(a) (b)

Fig. 22. (a) E-field distribution; (b) E-field intensity; glass based double slot structure.

place. The placing of slabs ensures slot width, substrate depth and cladding height. Such sort of triple slot structure has been checked for power confined inside low index slot region. Power confinement factor inside low index slot region is 30.75%. The simulations supported our earlier work for the case of glass based slabs with slots comprising of air.

Moving back to the case where glass based multiple slot structure is resting on glass substrate; cladding comprising of air. Two fifty nanometer wide slots separated using a central high index glass based slab of 50nm width; surrounded by 360nm wide slabs. Whole

structure resting on glass substrate, cladding is of air. Normalized E-field distribution and transverse E-field amplitude for a slot height of 1800nm is shown in figure 23 below.

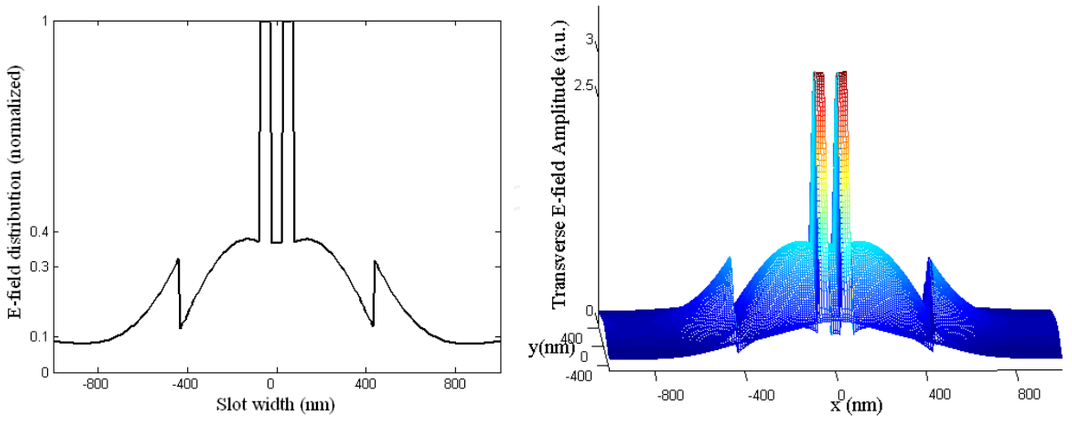

(a) (b)

Fig. 23. Normalized; (a) E-field intensity; (b) transverse E-field amplitude; glass based double slot structure.

Power confinement factor for glass based double slot structure has been investigated. For this check of power confinement factor inside low index slot regions, width of low index slot regions and central high index slab region was kept at 50 nm. Structure height was increased gradually from 300 nm till 1800 nm. Power confinement factor increases monotonously along with an increase in structure height (see figure 24 below).

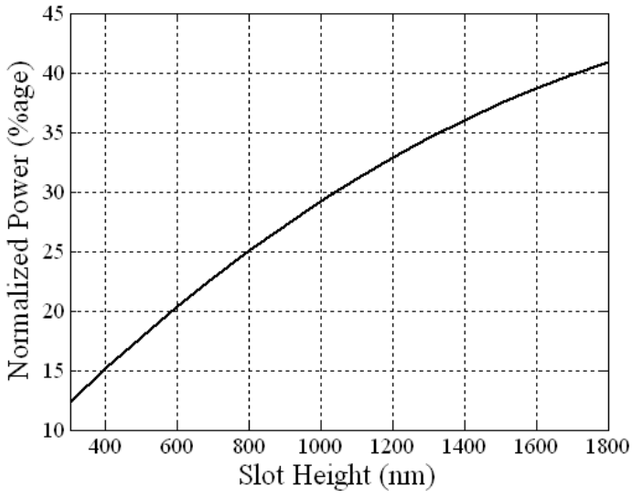

Fig. 24. Power confined in glass based double slot structure versus structure height.

Contrast ratio for SOI based slot structure is 2.42; power confined inside low index slot region for SOI based slot structure is approximately 60%. For a glass based slot structure contrast ratio is 1.65, attaining 41% power confinement factor inside low index slot regions brings the structure comparable to SOI slot structure. Glass based double slot structure is explored further for use in sensing applications.

5.1 Glass based Double Slot Structure Sensor [20]

In one of the example embodiment both 50nm wide slots are separated by a 50nm wide high index slab comprising of glass. Both slots separated by glass slab are surrounded by 360 nm wide glass slabs. The simulations scenario was created to calculate stress induced movement of center slab at one end of a long cantilever based sensor system [10]. Center slab is simulated to move (under the action of external pressure) by a step size of 5 nm each. Power confined in left slot is increasing; starting with a left slot width of 5 nm, center 50 nm glass slab is shifting right by a step of 5 nm. The left slot width is increasing by 5 nm whereas right slot width is reducing by 5 nm at each step size. Power confinement factor in both slots is same at equal width (50 nm).

It was found that power confinement factor is showing considerable change for a step size of 10 nm but for a step size of 5 nm the change is not considerable. This supports our earlier work done regarding high refractive index fluid based photonics displacement sensor.

Power confinement factor has been calculated for the case where; 50 nm slab is shifting right by a step size of 10 nm. In the start the left slot width is 5 nm, whereas right slot width is 95 nm. Results are displayed in figure 25. Power confinement factor is showing a considerable change for a shift in center slab by 10 nm; hence it can be exploited for forming a novel photonic displacement sensor.

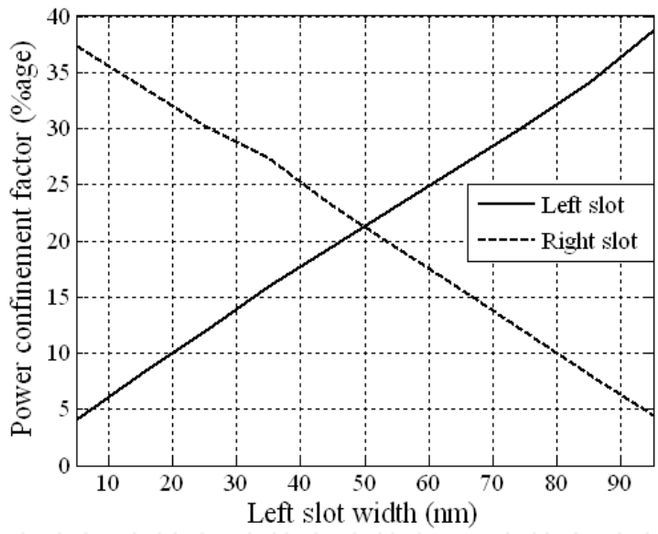

Fig. 25. Power Confinement factor in left slot region (center slab shifting right by 10nm).

5.2 Waveguide Structure

A displacement sensor based on double slot waveguide structure is designed. The structure comprising of compressible low refractive index material and hard material of relatively high index of refraction. Two low refractive index narrow slots formed between three relatively high refractive index slabs. The width of both slots and central slab is same.

The structural geometry can be changed as per requirements and designs. Figure 26 is a top view representation of double slot waveguide structure based photonics sensor. It is formed of slabs comprising of high refractive index hard material, having a width that can significantly be varied. Two low index slots comprising of low refractive index compressible

material separates the high refractive index slabs by a width, which is of the nanometers range. Low refractive index slot regions may be filled with air, gas, fluid or other compressible fluids so as to allow free movement of center slab in it. High refractive index regions may be filled with relatively high refractive index glass, silicon, silicon dioxide or metal. The height of high index slab regions also defines the height of low index slot regions. The length of high index slab regions also defines the length of low index slot regions. Central high index slab has an embedded fin on it's top, force on fin's vertical surface due to physical quantities makes the center slab move like a cantilever; left or right. Cladding of the structure are of same low refractive index material as of low index slot regions; further embodiments can be comprising of air, gas, fluid or other oxides.

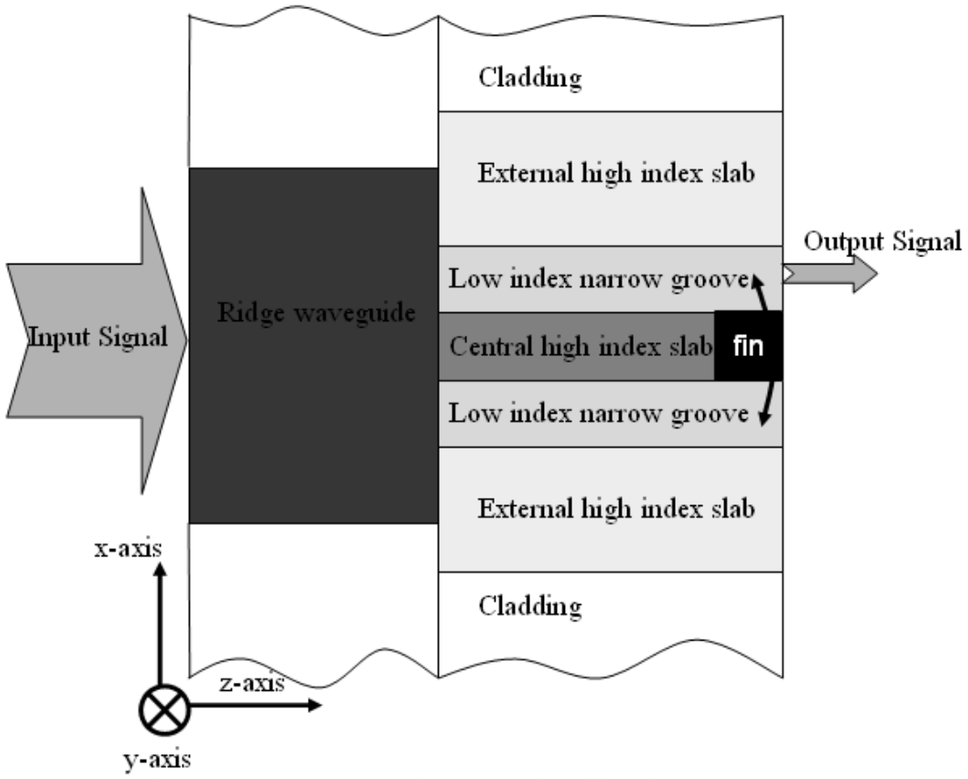

Fig. 26. Glass based photonics displacement sensor (top view; z-cut).

A channel waveguide structure is used for guiding light inside the double slot waveguide structure. Channel guide could be comprised of dielectric or any material of suitable refractive index, could be same as of high index slab regions or low index slot regions. Cladding of channel waveguide structure could be of same material as of double slot structure or could be of air, gas fluid or other metals / oxides. Another channel waveguide structure is used for directing light out of the double slot waveguide structure. The structural limitations are the same as for the earlier channel waveguide structure.

Low index slot regions may be supported by same material as used for the slabs. Other materials providing a contrast in refractive indices may also be utilized without departing from the scope of the invention. Many different structures may be used that provide a class of waveguide structures capable of guiding and confining lights in such a way that high

optical intensity is obtained in both small cross sectional areas filled with any compressible material of sufficiently low refractive index, relative to the remainder core of the structure. While low index slot regions are shown as a rectangular cross section, other shapes, such as triangular or semicircular may also be used to provide suitable surfaces for defining the narrow slot regions.

5.3 Working Principle

Light is guided inside double slot structure using a conventional waveguide (channel waveguide). The height of channel waveguide structure is same as that of double slot structure. Input field was coupled with the channel waveguide and later channel waveguide forming an integral part of double slot structure is a source of guiding light in it.

Referring figure 26, the central high refractive index slab is acting as a cantilever. Surface stress on fin on the top of central slab results in its' static bending. Displacement of central slab (cantilever) under the action of stress reduces the width of one of the slot resulting in increased width of other slot. Power confined inside low index slot is directly related to the width and hence is changed accordingly. Light is directed outside the double slot waveguide structure using an embedded channel waveguide structure.

In an example embodiment of glass based photonics sensor; using glass (high refractive index slab) and air (low refractive index slot). Referring figure 26, upper slot; hereafter named as right slot and lower slot; hereafter named as left slot, are of rectangular shape with 50 nm width, 1800 nm height and 1000 nm length comprising of air (R.I.=1.00). Upper slab; hereafter named as left slab, central slab and lower slab; hereafter named as right slab surrounding both low index slot regions. Slabs comprised of commercially available high refractive index glass (R.I. = 1.65); center slab width is same as that of low index slot regions; where as outer slabs width is 360nm. Input plane is propagated along z-axis at 1.55 μm CW (optical frequency).

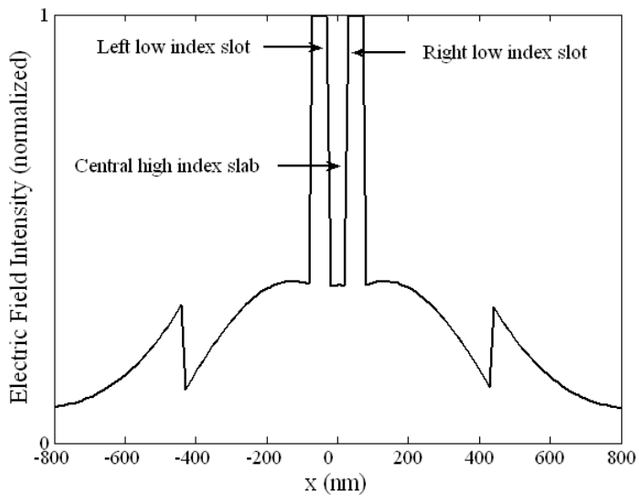

Fig. 27. (a): Normalized E-field intensity – both low index slot regions of same width.

The shift in center slab with a step size of 10 nm is causing a constant increase in left slot width starting from 5 nm till 95 nm; vice versa constant decrease in right slot width. Power

confinement factor is directly proportional to the slot width. Change in power confinement factor is being used as an indicator for shift in displacement of center slab. Normalized E-field intensity in double slot waveguide structure is displayed in figure 27 (a), (b) & (c) at three different displacement locations of center slab.

In this embodiment example (see Fig. 27(a)), E-field intensity has been calculated by keeping both slots at same width. As the slots width was same, hence power confined in both slots is same. Power confinement has been calculated using Eqn. 3 [3] and it was found same. Figure 27(a) above gives a very nice example of double slot waveguide structure, where quasi-TE mode is used. Light is totally confined inside the low index slot region. E-field was normalized with it's peak value. The E-field distribution at modal point depends upon the input conditions and geometrical shapes of slot waveguide structure. The input conditions and refractive index contrast were kept same; however geometrical conditions were changed in further embodiments. The change in geometrical conditions due to shift in central slab has a profound effect on the E-field distribution at the modal points. We will see in figures below that, for the embodiment where left low refractive index slot width is less; E-field confinement is high.

In this embodiment example (see Fig. 27(b)), numerical calculations have been done by keeping left low refractive index slot width at 5 nm. Right low refractive index slot width was 95 nm (vice versa). E-field was normalized with the E-field obtained when both the slots width is same (see fig. 27(b) below). It is evident from the figure that power was mainly confined in right low refractive index slot. Power confinement factor in both low refractive index slots has been calculated using Eqn. 3 [3].

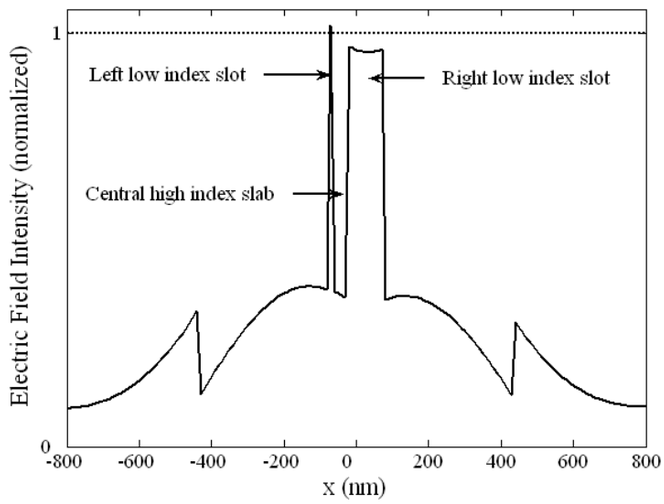

Fig. 27. (b): Normalized E-field intensity – left slot of width 5nm; right slot of width 95nm.

In this embodiment example (see Figure 27(c)), numerical calculations have been done by keeping left low refractive index slot width at 95 nm. Right low refractive index slot width was 5 nm (vice versa). E-field was normalized with the E-field obtained when both the slots width is same (see figure 27(c) below). It is evident from figure; that power was confined in left low index slot. However sharp spike of light confinement in right low refractive index groove is due to it's small cross sectional area. Power confinement factor in both low refractive index slots has been calculated [3]. The large cross sectional area of left slot

attributed towards high power confinement; vice versa right low refractive index slot contains less power.

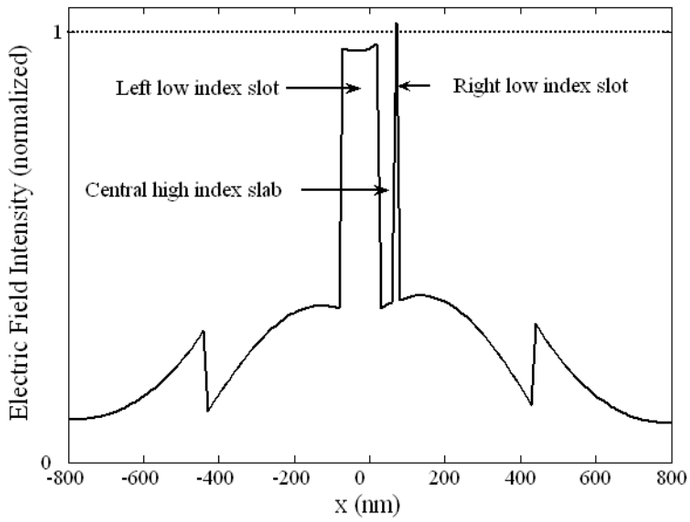

Fig. 27. (c): Normalized E-field intensity – right slot of width 5nm; left slot of width 95nm.

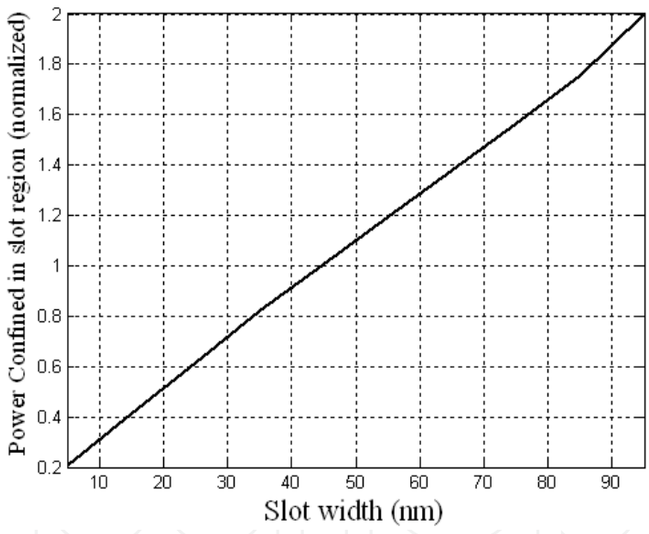

Fig. 28. Power confined (normalized) inside low refractive index slot region dependence upon slot width.

Power confined in either low index slot region is increasing along with increase in slot width. The low index slot width is dependent upon shift in center slab. Power confinement factor in both low index slots have been checked and found similar response at same displacement of central high refractive index slab. Power confined (normalized) in a low index slot region has been drawn in graphical format in figure 28. The change in slot width is due to shift in center slab under the effect of stress at fin's vertical surface. We have checked the power confinement factor at various example embodiments. Few power

confinement values plotted in figure 28 are just for example. It was observed that in order to get a considerable change in power confinement factor a minimum shift of 10nm in center slab width is required. A shift in power confinement factor by 3.85 has been found for every 10nm change in center slab displacement. Hence sensitivity of proposed photonics sensor mechanism is 0.385/nm.

6. Slot Structure Coupling Structures

In order to ensure usage of glass based low contrast slot structure in forming passive optical devices, it was necessary to provide an example. Slot waveguide based single slot to double slot coupling structure (see figure 29) is realized using glass & air based single and multi slot structure.

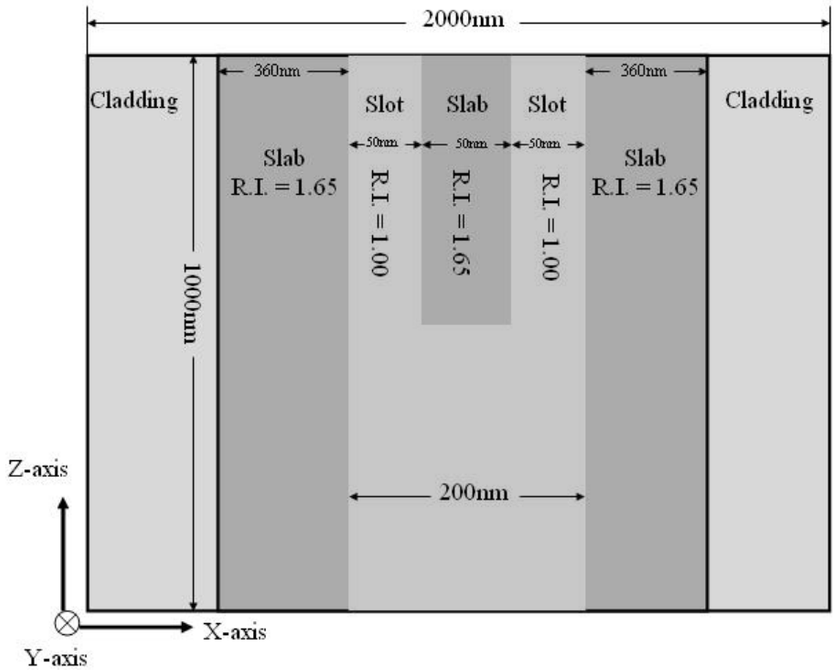

Fig. 29. Slot waveguide based Y-coupler.

In a numerical calculation using full vector finite difference mode-solver, the dimensions of double slot structure as follows:
Referring figure 29, both slots are of rectangular shape with 50 nm width, 400 nm height and 1 μm length comprising of air (R.I.=1.00). Three rectangular slabs are surrounding both the slots comprising of commercially available high refractive index glass (R.I. = 1.65). Single frequency Gaussian modulated continuous wave was used as input plane, propagated in the direction of z-axis. Numerous numerical calculations by using standard input plane were carried out at various displacement values. E-field amplitude shows that a part of optical power is also in the substrate. However due to electric field discontinuity at the boundaries of high index glass slabs and low index air slots, the e-field is confined strictly inside the low index regions. However contrast ratios do have an effect on the power

confinement factor. This effect has been nullified by changing the structure geometry and changing the input plane conditions.
Referring figure 29; initially basic SOI slot optical waveguide was simulated [1]. The light was confined inside low index regions (see figure 30) and is in agreement with the existing theory.

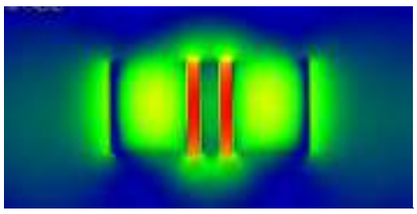

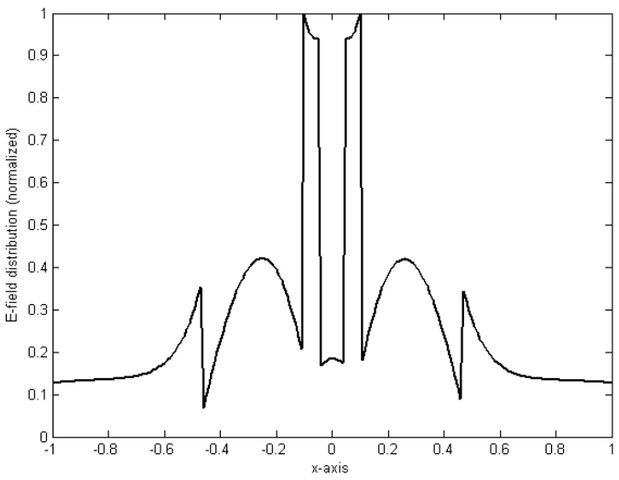

(a) (b)

Fig. 30. (a) E-field distribution; (b) E-field intensity; SOI slot optical waveguide based Y-branch coupler.

Glass based double slot waveguide structure is implemented on the Y-branch coupler model. The slots comprising of air and slabs is of glass. E-field distribution is plotted in figure below:

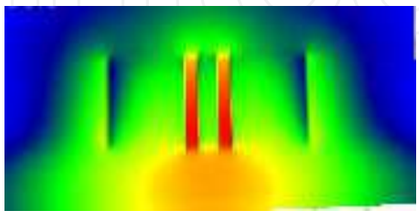

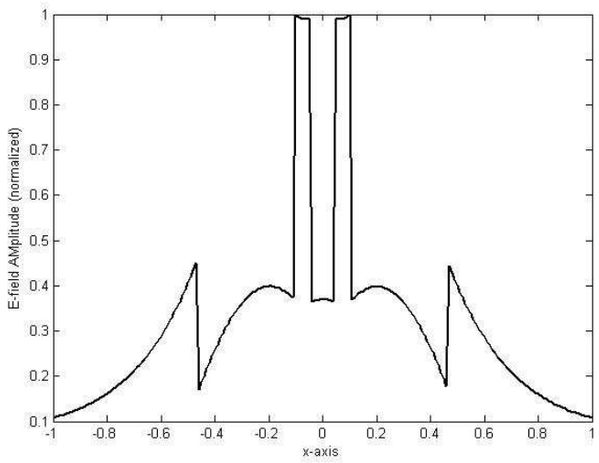

(a) (b)

Fig. 31. (a) E-field distribution; (b) E-field intensity; Double slot waveguide structure (comprising of air & glass) based Y-coupler.

E-field intensity is found splitting into two parts, hence power introduced in the y-branch coupler is splitted equally in between two ports. This is very useful in forming passive optical devices. It can be further exploited in forming complex passive optical devices.

7. Summary

In this chapter simulation and analysis of single and multiple slot waveguide structures had been carried out using FDTD algorithm. It was found that multiple slot structures not only increase the power confinement factor in low index slot regions but can also be utilized in forming sensor mechanisms. Other than traditional SOI slot optical waveguides, low contrast (glass and air based) slot optical waveguides with comparable power confinement factor had been proposed. Later the low contrast double slot optical waveguide structure had been utilized in forming cantilever based sensing mechanisms. Light confinement inside low contrast double slot structure has been explored and found comparable to SOI based slot optical waveguide structure. Based on cantilever type movement of low index slots of proposed low contrast double slot structure a simple and easy to build optomechanical sensor has been proposed. Single frequency continuous wave Gaussian pulse source has been used in simulations which is readily available. It could be most probable candidate for use in temperature, pressure and surface smoothness sensing.

8. References

[1] V. R. Almeida, Q. Xu, and M. Lipson et. al., "Guiding and confining light in void nanostructure," Optics Letters, 2004, vol.29, no.11, p.1209-1211.

[2] Q. Xu, V. R. Almeida, and M. Lipson et. al., "Experimental demonstration of guiding and confining light in nanometer-size low-refractive-index material," Optics Letters, 2004, vol. 29, no.14, p.1626-1628.

[3] N. N. Feng, J. Michel, and L. C. Kimerling, "Optical field concentration in low-index waveguides," IEEE Journal of Quantum Electronics, 2006, vol.42, no.9, p.885-890.

[4] T. Fujisawa and M. Koshiba, "All-Optical Logic Gates Based on Nonlinear Slot Waveguide Couplers," Journal of Optical Society of America B, 2006, vol.23, p.684-691.

[5] K. K. McLauchlan, S. T. Dunham, "Analysis of a Compact Modulator incorporating a hybrid silicon/electro-optic polymer waveguide," IEEE Journal of selected topics in Quantum Electronics, 2006, vol.12, no.6, p 1455-1460.

[6] P. A. Anderson, B. S. Schmidt, and M. Lipson, "High confinement in silicon slot waveguides with sharp bends," Optics Express, vol.14, no.20, 2006, p.9197-9202.

[7] R. Hainberger and P. Mullner, "Modal behavior of SOI slot waveguides," Proceedings of Symposium on Photonics Technology for 7th Framework Program Wroclaw, 2006, p.282-285.

[8] P. Mullner and R. Hainberger, "Structural optimization of silicon-on-insulator slot waveguides," IEEE Photonics Technology Letters, 2006, vol.18, no.24, p.2557-2559.

[9] N. N. Feng, R. Sun, and L. C. Kimerling et. al., "Lossless strip-to-slot waveguide transformer," Optics Letters, 2007, vol.32, no.10, p.1250-1252.

[10] C. A. Barrios, "Ultrasensitive nanomechanical photonic sensor based on horizontal slot waveguide resonator," IEEE Photonics Technology Letters, 2006, vol.18, no.22, p.2419-2421.
[11] F. D. Olio, and V. M. N. Passaro, "Optical sensing by optimized silicon slot waveguides," Optics Express, 2007, vol.15, no.8, p.4977-4993.
[12] P. Sanchis, J. Blasco, and A. Martinez et. al., "Design of silicon based slot waveguide configurations for optimum nonlinear performance," Journal of Lightwave Technology, vol. 25, no. 5, 2007, p. 1298-1305.
[13] T. Fujisawa, and M. Koshiba, "Guided modes of nonlinear slot waveguides," IEEE Photonics Technology Letters, 2006, vol.18, no.14, p.1530-1532.
[14] L. Chen, J. Shakya, M. Lipson, "Subwavelength confinement in integrated metal slot waveguide on silicon," Optics Letters, 2006, vol.31, no.14, p.2133-2135.
[15] J. A. Dionne, H. J. Lezec, H. A. Atwater, "Highly confined photon transport in subwavelength metallic slot waveguides," Nano Letters, 2006, vol.6, no.9, p.1928-1932.
[16] M. Iqbal, Z. Zheng, and J. S. Liu, "Light confinement in multiple slot structures investigated," Proceedings of IEEE, ICMMT Nanjing China, ISBN- 978-1-4244-1879-4, 2008, p.878-891.
[17] Z. Zheng, M. Iqbal, and JS Liu, patent application launched to Chinese Govt.
[18] M. Iqbal, Z. Zheng, and J. S. Liu, "Low contrast double slot structure based optomechanical sensor," Submitted for presentation in Asia Pasic Optical Conference, 09, Shanghai, China.
[19] High refractive index fluids. http://www.2spi.com/catalog/ltmic/cargille-liquid.html
[20] M. Iqbal, Z. Zheng, and J. S. Liu, "Low Refractive Index Contrast Double Slot Structure Based Cantilever Type Sensor," Submitted for presentation in Asia Pasic Optical Conference, 09, Shanghai, China.

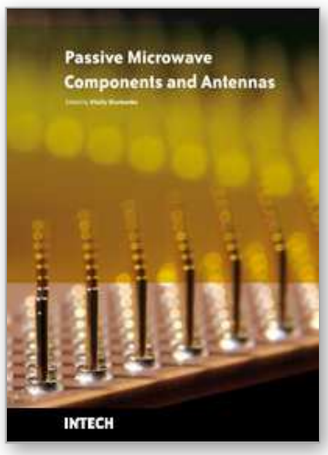

Passive Microwave Components and Antennas

Edited by Vitaliy Zhurbenko

ISBN 978-953-307-083-4
Hard cover, 556 pages
Publisher InTech
Published online 01, April, 2010
Published in print edition April, 2010

Modelling and computations in electromagnetics is a quite fast-growing research area. The recent interest in this field is caused by the increased demand for designing complex microwave components, modeling electromagnetic materials, and rapid increase in computational power for calculation of complex electromagnetic problems. The first part of this book is devoted to the advances in the analysis techniques such as method of moments, finite-difference time- domain method, boundary perturbation theory, Fourier analysis, mode-matching method, and analysis based on circuit theory. These techniques are considered with regard to several challenging technological applications such as those related to electrically large devices, scattering in layered structures, photonic crystals, and artificial materials. The second part of the book deals with waveguides, transmission lines and transitions. This includes microstrip lines (MSL), slot waveguides, substrate integrated waveguides (SIW), vertical transmission lines in multilayer media as well as MSL to SIW and MSL to slot line transitions.

InTech Europe
University Campus STeP Ri
Slavka Krautzeka 83/A
51000 Rijeka, Croatia
Phone: +385 (51) 770 447
Fax: +385 (51) 686 166
www.intechopen.com

InTech China
Unit 405, Office Block, Hotel Equatorial Shanghai
No.65, Yan An Road (West), Shanghai, 200040, China
中国上海市延安西路65号上海国际贵都大饭店办公楼405单元
Phone: +86-21-62489820
Fax: +86-21-62489821

IntechOpen